# Thermocurable Hyperbranched Polystyrenes for Ultrathin Polymer Dielectrics

**Jeong Ae Yoon, Tomasz Young, Krzysztof Matyjaszewski,* and Tomasz Kowalewski***

Center for Macromolecular Engineering, Department of Chemistry, Carnegie Mellon University, 4400 Fifth Avenue, Pittsburgh, Pennsylvania 15213

**ABSTRACT** Thermocurable hyperbranched polystyrenes were successfully synthesized using atom transfer radical polymerization and exhibited superior ultrathin film formation capabilities in comparison with the linear analogues, as assessed by the minimal film thickness attainable by spin-coating without dewetting. They were suitable as ultrathin film organic dielectrics, with parallel plate specific capacitances as high as ~680 nF/cm$^2$. Similar to high performance inorganic dielectrics, capacitance measurements pointed to the presence of "dead" interfacial capacitance, which could be accounted for by considering the geometric effect of roughness "incommensurability" between metal electrode and polymer film.

**KEYWORDS:** hyperbranched polymer • ultrathin film polymer dielectrics • dead interfacial capacitance • atomic force microscopy • ATRP

## INTRODUCTION

One of the particularly interesting applications of ultrathin polymer films is their use for surface modification of materials without changing substrate bulk properties. Examples of surface modifications accomplished in this manner include changing surface properties, such as wettability by particular liquids or biocompatibility (1−5), as well as the introduction of additional properties such as chemical reactivity, photosensitivity, electrical conductivity, magnetic properties, etc. (6−11).

Ultrathin films have been fabricated by physical methods such as dip coating, spin coating, or Langmuir−Blodgett techniques as well as by chemical methods such as grafting techniques (12−17). Among physical methods, the spin coating method is particularly popular because it is applicable to virtually all solution-processable polymers and the film thickness can be easily controlled by solution concentration or spinning speed. However, spin coated films with thicknesses below few nanometers, i.e., thinner than the effective size of polymer coil, are often unstable and spontaneously dewet (18, 19). Although under the high shear force of spin coating, polymer coils can be stretched in the plane of the film to accommodate the desirable thickness, this stretching will be countered by the entropic elasticity forces attempting to restore the equilibrium chain conformation. This leads to dewetting, unless the polymer chains are immediately stabilized, e.g., by anchoring to the substrate or by cross-linking (2, 20−23). Herein we demonstrate that the undesirable dewetting can be reduced through the use of highly branched (24, 25), cross-linkable polymers, presumably because of their more compact shape (26, 27), allowing achievement of lower thickness without extensive coil stretching (Scheme 1).

Specifically, we focus on the preparation and use of hyperbranched copolymers based on polystyrene and 3-(trimethoxysilyl)propyl methacrylate (28, 29). The controlled/"living" radical polymerization (CRP) (30−32) was employed to avoid unwanted macroscopic gelation during polymerization, resulting in hyperbranched structures (33−35). Atom transfer radical polymerization (ATRP) (36−40) and activators regenerated by electron transfer (ARGET) ATRP (41−43) were used for this purpose. Branching points were provided by the AB* inimer (i.e., molecule containing both polymerizable moiety A and bromine initiator fragment B*), α-bromoisobutyryloxyethyl methacrylate, and/or by the divinyl cross-linker, divinylbenzene. Cross-linking of the film and its covalent anchoring to the substrate were made possible through the incorporation of trimethoxysilyl groups, capable of undergoing hydrolysis and subsequent polycondensation to form siloxane linkages. Comparison of ultrathin film forming capabilities of hyperbranched polymers with linear analogues confirmed the anticipated advantages of hyperbranched structures. Moreover, dielectric measurements performed with cross-linked hyperbranched polymer films demonstrated their suitability for application as ultrathin polymer dielectrics.

## RESULTS AND DISCUSSION

The thermocurable hyperbranched polystyrenes were synthesized by self-condensing vinyl copolymerization (SCVcP) of styrene (St) and 3-(trimethoxysilyl)propyl methacrylate (TMSPMA) in the presence of 2-bromoisobutyryloxyethyl methacrylate (BIEM) and/or divinylbenzene (DVB) (Scheme 2). In principle, it is possible to prepare vinyl monomer-based hyperbranched polymers by adding very low amount of multivinyl cross-linkers using free radical polymerization mechanisms. However, under conventional

* Corresponding author. Tel: (412) 268-5927 (T.K.); (412) 268-3209 (K.M.). Fax: (412) 268-1061 (T.K.); (412) 268-6897 (K.M.). E-mail tomek@andrew.cmu.edu (T.K.); km3b@andrew.cmu.edu (K.M.).

Received for review May 26, 2010 and accepted July 26, 2010

DOI: 10.1021/am100463z

**Scheme 1. Proposed Mechanism of Anticipated Improvement of Ultrathin Film Forming Capabilities of Hyperbranched vs Linear Polymer**[a]

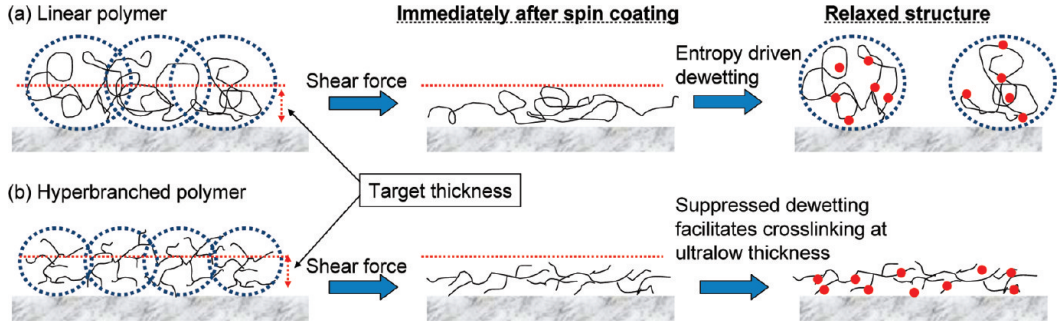


[a] Blue dotted circles represent effective random coil sizes of polymers; red dots represent siloxane linkages. While hyperbranched polymer maintains the stretched form sufficiently long enough for cross-linking reaction to occur, linear polymer dewets before the film stabilization by cross-linking.

**Scheme 2. Synthesis of a Thermocurable Hyperbranched Polystyrene-*co*-poly(3-(trimethoxysilyl)propyl methacrylate)**

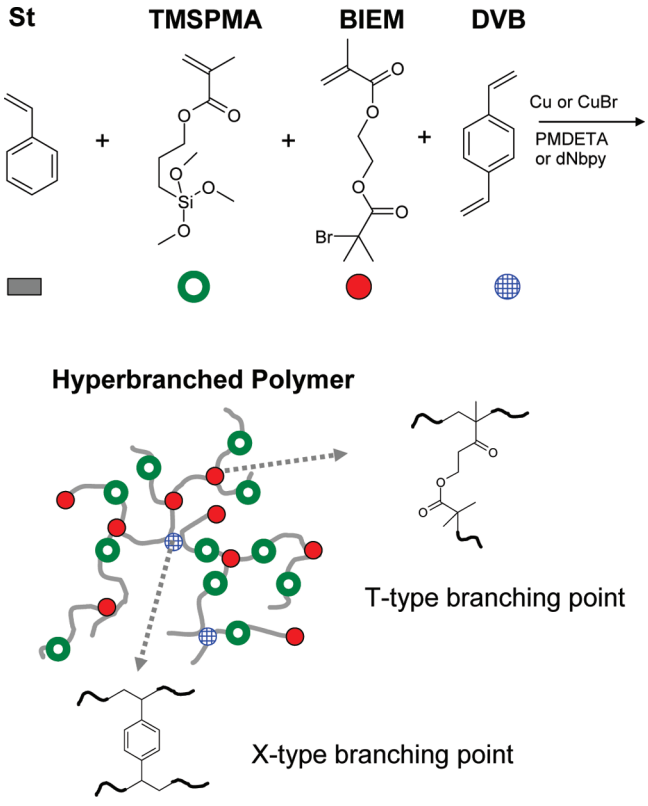


free radical polymerization conditions, gel point prediction is very difficult and undesired macroscopic gelation often occurs while preparing hyperbranched polymers, unless chain transfer agent (CTA) is added at the ratio of [cross-linker]/[CTA]≤1, to an adequately diluted reaction medium (44−46). In the present study, uncontrolled macroscopic gelation was avoided by using controlled radical polymerizations, such as ATRP and ARGET ATRP.

Formation of hyperbranched structure was achieved through the incorporation of two types of branching moieties. Incorporation of BIEM into growing chains facilitated formation of branches by grafting-from approach, leading to the formation of "T-type" branches (47, 48). In addition, DVB, which at higher concentrations could act as a cross-linker, facilitated the formation of "X-type" branching points by linking different growing polymer chains. In the SCVcP synthesis of hyperbranched polymers based solely on "T-type" branching agents (inimers), the molecular weights, $M_w/M_n$, and the degree of branching (DB) increase with the monomer conversion. When the ratio of inimer to monomer is low, as in the present study (dilution factor $\gamma$ = [monomer]/[inimer] = 20), the inimer is consumed rapidly at a low monomer conversion, and the early stage of polymerization resembles a living polymerization process for linear chains. Subsequently, linkage reactions of polymeric chains lead to the formation of branches and the molar mass increases more rapidly. According to literature, the maximum degree of branching (reached upon full monomer conversion) is approximately equal to $2/\gamma$ (49). For the system studied here ($\gamma$ = 20), this would yield a relatively low value of DB = 0.1. To increase this value, we used the additional "X-type" branching agent.

TMSPMA was used to introduce a thermocurable functionality into the copolymer. Hydrolysis and consecutive polycondensation of trimethoxysilyl groups yielded polysiloxane cross-links (28, 29). Polymers prepared under various synthetic conditions are listed in Table 1. Since preliminary studies revealed that polymers with weight average molecular weights ($M_w$) below 10,000 tended to dewet during cross-linking at 80 °C (see the Supporting Information), presumably due to sufficient degree of intermolecular entanglement, all subsequent work has been focused on the systems with molecular weights exceeding this value. Successful cross-linking of the films was confirmed by checking their resistance against exposure to toluene (which was used as polymer solvent during film preparation), assessed by ellipsometric thickness measurements and AFM observations before and after solvent exposure. Detailed description and discussion of all important aspects of molecular design, synthetic procedures, and sample preparation/testing conditions are provided in Supporting Information.

Ultrathin film forming and dielectric properties were compared for two hyperbranched copolymers (AP1C and RP1C) with maximized degree of branching, and their linear analogues. Polymer solutions of various concentrations (0.01−0.2 % in toluene) were spin-cast on a silicon wafer to prepare films of different thicknesses. The film thicknesses

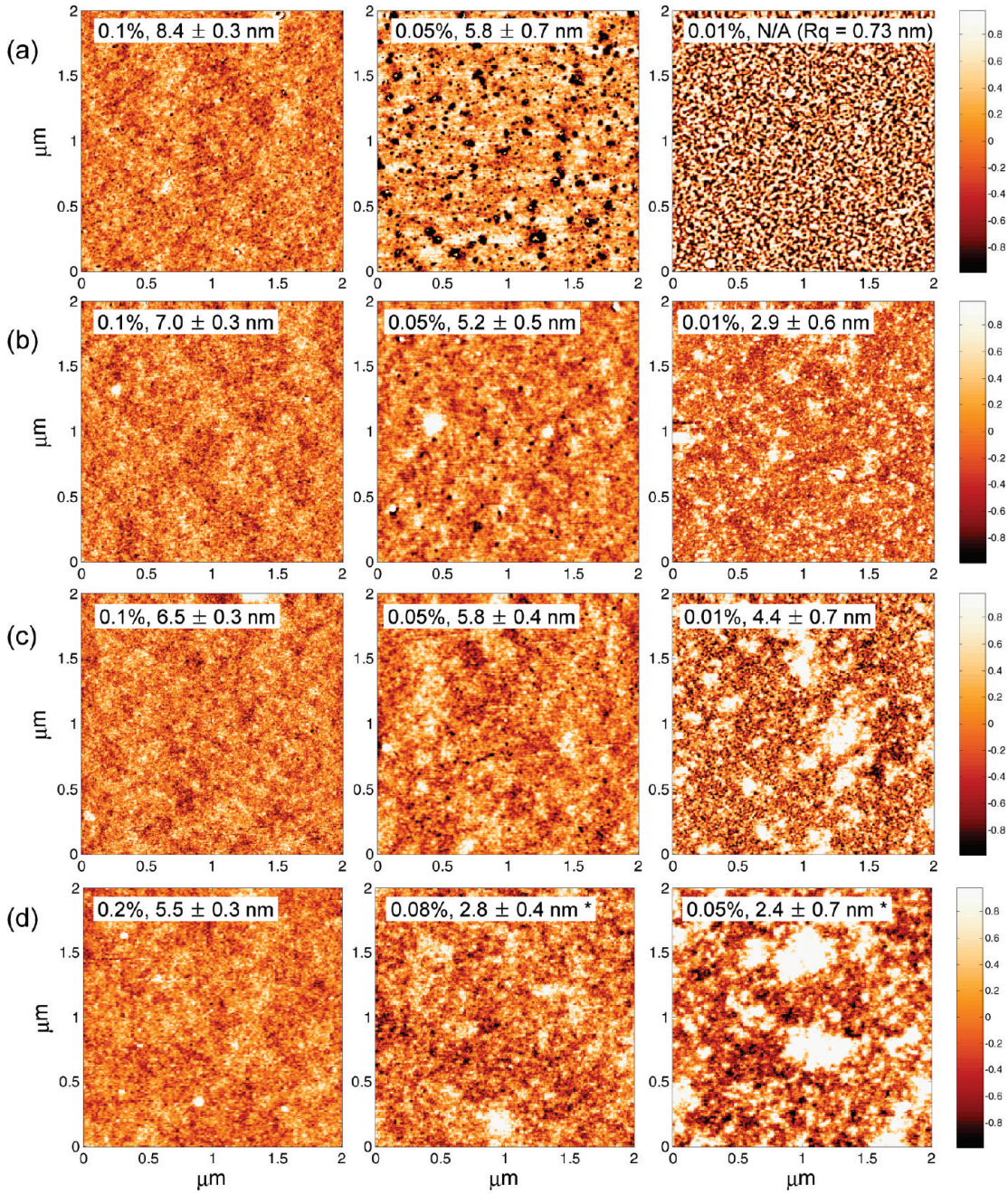


**FIGURE 1. Comparison of ultrathin films formed by linear and hyperbranched polymers. Numbers in rectangular boxes are solution concentration (wt/vol %) and thickness (nm), respectively. * The thicknesses were measured by contact mode AFM. The other samples were measured by ellipsometry ($n = 3$). The error ranges are the rms roughness values ($R_q$) calculated from the AFM images. The films were cross-linked at 80 °C, overnight. Coating: 4000 rpm, 2 min. (a) Linear polymer, L; (b) hyperbranched polymer, AP1C; (c) hyperbranched polymer, RP1C; (d) hyperbranched polymer, RP1C (solution was dropped on the spinning substrate).**

were measured by ellipsometry or contact mode AFM (Supporting Information) and the surfaces of the films were imaged using tapping mode AFM (Figure 1). For all polymers, films with thicknesses in the range of 6.5 to 8.5 nm were smooth and continuous with root-mean-square (rms) roughness Rq ~ 0.33 nm (Figure 1a–c, left). The formation of dewetting related defects became evident, once the film thickness was reduced to 5–6 nm (Figure 1a–c, center). Those defects had the form of "pinholes" and were particularly numerous in the linear polymer sample, with only few scattered defects observable in hyperbranched polymer films. Upon a further decrease in thickness, linear polymer films underwent dewetting that was manifested through the presence of characteristic reticulated morphology (Figure 1a, right). Importantly, hyperbranched polymer films cast from the similar solution concentrations still maintained their integrity while reaching the thickness of ~3–4 nm although their rms roughness was markedly higher in comparison with thicker films (0.7 nm vs 0.3 nm). This result demonstrates that hyperbranched architecture indeed offers advantages when it comes to reducing the thickness of spin-coated films. The observed increase in roughness upon reduction of film thickness down to ~3–4 nm may be a consequence of some "disentanglement" between hyper-

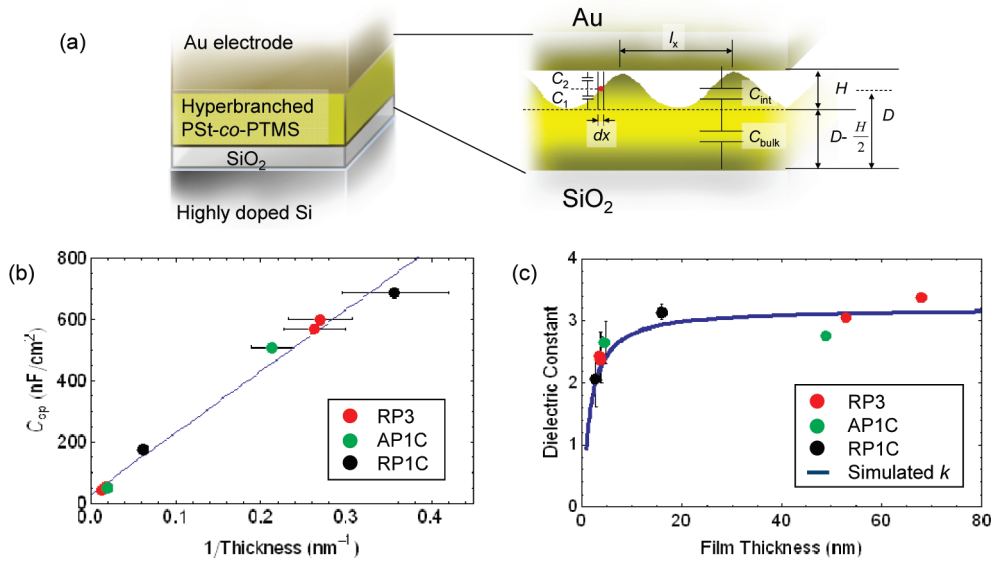


**FIGURE 2. Dielectric measurements of ultrathin polymer films. (a) Sample geometry and the model proposed to illustrate the connection between the "dead" layer capacitance and roughness "incommensurability" between Au and polymer surface. (b) Specific capacitance of parallel-plate capacitors containing the synthesized hyperbranched polymers as the dielectrics (1 kHz sinusoidal probing signal with the amplitude of 100 mV). (c) Comparison of apparent dielectric constants calculated from the $C_{sp}$ (symbols) with the values predicted by the model shown in (a) (continuous line).**

branched molecules. Because this thickness range becomes comparable with effective diameters of individual hyperbranched molecules, large variability of thickness (high surface roughness) may be also reflecting the distribution of molecular weights. One could argue that if "disentanglement" is an issue, some improvement in film uniformity could be achieved by casting from more concentrated solutions. To explore this possibility, we prepared films of polymer RP1C by spin-casting from solutions which were 2−5 times more concentrated. Achievement of ≲5 nm thickness required alternative solution delivery mode in this case; rather than depositing solution on the resting wafer and then ramping the rotational speed up to 4000 rpm, the 20 $\mu$L droplets were deposited directly onto the substrates rotating at 4000 rpm. As evident from AFM images of such prepared films (Figure 1d), the only effect of such change in the deposition procedure was the reduction of the incidence of infrequent pinholes observed earlier at the thickness of ∼5 nm (c.f., center images in Figure 1c,d). Sub-5 nm films still exhibited increased rms roughness ( 0.7 nm), perhaps indicating that this roughness increase was due to the polymer polydispersity rather than "disentanglement".

Performance of films prepared from hyperbranched polymers as ultrathin polymer dielectrics and comparison of their dielectric properties with "bulk" properties were characterized by means of simple capacitance measurements. Parallel-plate capacitors were fabricated by vapor-depositing circular gold electrodes (2 mm in diameter) on top of the films residing on highly doped silicon substrates which served as a second capacitor plate (Figure 2a). Capacitance of such prepared samples was measured using a capacitance bridge using 1 kHz sinusoidal probing signal with the amplitude of 100 mV. Because film thickness was comparable to the thickness of native oxide (2.4 nm by ellipsometry) on the silicon wafer, the results were corrected for the resulting series capacitance of oxide layer. The resulting plot of specific capacitance ($C_{sp}$) vs reciprocal film thickness ($1/d$) is shown in Figure 2b. The highest specific capacitance of 680 nF/cm$^{-1}$ was obtained with the thinnest film ($d = 2.8$ nm). At the first inspection, the plot appears to follow the simple linear relationship, as expected for a parallel-plate capacitor, however the dielectric constant of the material obtained through linear regression ($k = 2.3 \pm 0.1$) was outside of the error limits lower than the value expected for polystyrene matrix ($k = 2.5$) containing siloxane linkages. This prompted re-evaluation of data through point-by-point calculation of dielectric constants for each film thickness, results of which are shown in Figure 2c. On the basis of this analysis, the dielectric constant of samples with thickness greater than ∼10 nm did not appear to vary systematically with thickness and was equal to 3.1 ± 0.3. In contrast, for thinner films, its value decreased almost linearly from 2.7 to 2.2. Importantly, the value of $k$ in the thickness independent regime was indeed higher than one known for polystyrene, as expected given the presence of siloxane and methacrylate groups in the material. It should be noted that the similar drop of apparent dielectric constant has been widely reported in the literature on thin film capacitors based on high-$k$ dielectrics and ferroelectric materials, and is recognized as one of the challenges in fabrication of high-performance nanocapacitors (50). The significant deviations from the bulk are observed for film thicknesses below a few tens of nanometers (as in the case described herein), and are often attributed to the presence of a "dead" interfacial capacitance connected in series with the bulk of the film. Currently there is a debate whether the origin of the dead layer is related to interfacial defects (e.g., grain boundaries (51), stresses (52), interface states (53), contaminants (52)) or if it is an intrinsic property of metal−dielectric interface (50). As discussed below, in our

**Table 1. Linear and Hyperbranched Thermocurable Polystyrenes by ATRP or ARGET ATRP**

| entry[a] | mechanism | composition[b] | catalyst | Conv[c] (%)/time (h) | $M_n$, $M_w$, $M_w/M_n$[f] |
|---|---|---|---|---|---|
| **L** | ATRP | St:TMSPMA:EBiB:Cu(I) 100:10:0.25:0.25 | CuCl/PMDETA | 40/25[d] | 23500, 30500, 1.30 |
| **AP1** | ATRP | St:TMSPMA:BIEM:Cu(I) 100:10:5.5:0.55 | CuBr/PMDETA | 82/68[e] | 7700, 13200, 1.72 |
| **RP1** | ARGET | St:TMSPMA:BIEM:Cu(0) 100:10:5.5:0.55 | Cu(0)/PMDETA | 90/30[e] | 7900, 16500, 2.09 |
| **RP3** | ARGET | St:TMSPMA:BIEM:Cu(0) 100:30:6.5:0.65 | Cu(0)/PMDETA | 92/30[e] | 10100, 21100, 2.09 |
| **AB1** | ATRP | St:TMSPMA:BIEM:Cu(I) 100:10:5.5:0.55 | CuBr/dNbpy | 19/95[e] | oligomerization |
| **RB1** | ARGET | St:TMSPMA:BIEM:Cu(0) 100:10:5.5:0.55 | Cu(0)/dNbpy | 65/89[e] | 8600, 13600, 1.58 |
| **AP1C** | ATRP | St:TMSPMA:BIEM:DVB:Cu(I) 100:10:5.5:2.2:0.55 | CuBr/PMDETA | 85/64[e] | 15800, 68800, 4.36 |
| **RP1C** | ARGET | St:TMSPMA:BIEM:DVB:Cu(0) 100:10:5.5:2.2:0.55 | Cu(0)/PMDETA | 82/20[e] | 46300, 490000, 10.6 |

[a] L denotes linear polymer; for hyperbranched polymers, the first letter (A or R) refers to the procedure used to prepare the copolymer (ATRP or ARGET ATRP, respectively), the second letter (P or B) identifies the ligand used (PMDETA or dNbpy, respectively), the number (1 or 3) indicates the ratio of [TMSPMA]:[St] (10:100 or 30:100). Finally, if the cross-linker DVB was added to the reaction, the letter C was included as the last character. [b] For hyperbranched polymers, ([St]+[TMSPMA])/[BIEM] = 20, [BIEM]/[Cu/ligand] = 10, [PMDETA]/[Cu] = 1, and [dNbpy]/[Cu] = 2. When DVB was used, [DVB]/[BIEM] = 0.4. [c] Based on styrene conversion measured by GC. [d] 80 °C. [e] 90 °C. [f] GPC by linear PSt standard calibration.

case, the presence of the "dead" interfacial layer could be caused by "incommensurability" of intrinsic nanoscale roughness of polymer and gold films, leading to the formation of "nanoporous" interface, as shown schematically in Figure 2a. The primary source of such "incommensurability" would be the relatively large size of Au crystallites in comparison with the characteristic minimal length scale of roughness of the polymer film, as reflected in the power spectra of AFM images (see the Supporting Information, Figure SI8). Its effect on the value of $k$ has been estimated using a simple model in which "flat" Au surface is in contact with a sinusoidally rough polymer surface with rms roughness $\sigma$ corresponding to the value obtained from AFM measurements. In this model, the equivalent capacitance of the system is treated as a series connection of bulk capacitance ($C_{bulk}$) and interfacial layer capacitance ($C_{int}$). $C_{int}$ in turn comprises a distribution of parallel capacitors formed by a series connection of "air" and "bulk polymer" capacitors with thicknesses of air and polymer contributions varying according to the surface profile. Assuming the sinusoidal profile of polymer surface, the equivalent specific capacitance per unit area of the interfacial region can be calculated by integration over one period of a sinusoid and then combined with bulk specific capacitance. The ratio of the apparent dielectric constant of the material extracted from such obtained capacitance, $k_{app}$, to the bulk dielectric constant $k$ is then equal to

$$\frac{k_{app}}{k} = \frac{(2 - \alpha)}{2 - \alpha(1 - 2\sqrt{k})} \qquad (1)$$

where $\alpha$ is the parameter characterizing the relative surface roughness, $\alpha = 1.63\ (\sigma)/(D)$, and $\sigma$ and $D$ denote, respectively, rms surface roughness and overall film thickness measured from the bottom to the average height on the surface (Figure 2b).

It can be easily checked that in the limit when film roughness is small compared to film thickness ($\alpha \rightarrow 0$), $k_{app}/k$ tends to unity. For bulk dielectric constant $k = 3.1$, as for materials studied herein, the significant deviations from unity ($k_{app}/k \leq 0.9$) would appear when $\alpha \geq 0.061$ (i.e., $\sigma/D \geq 0.037$). Assuming that the roughness of a polymer film remains unchanged after metal deposition, and is equal to the typical value of observed in the present study ($\sigma \approx 0.5$ nm), deviations from bulk dielectric constant >10% should be then observed for films thinner than about 13 nm. This indicates that roughness effects could be invoked in the explanation of the observed discrepancies. As shown in Figure 2c, in which the thickness dependence of $k_{app}$ predicted by eq 1 is plotted together with the values of $k$ determined from capacitance measurements, the proposed simple geometric model could, in principle, fully account for the observed behavior.

In conclusion, thermocurable hyperbranched polymers were successfully synthesized using controlled radical polymerization techniques (ATRP and ARGET ATRP), and were shown to exhibit superior ultrathin film formation capabilities in comparison with the linear analogues. This was manifested in their significantly lower value of the minimal pinhole-free film thickness attainable by spin coating from solution (~3−4 nm vs ~8 nm for linear polymer). Suitability of such prepared hyperbranched polymer films as ultrathin film organic dielectrics was demonstrated through fabrication of parallel plate capacitors which specific capacitances as high as ~680 nF/cm$^2$, i.e., close to the highest values reported for organic dielectric capacitors based on self-assembled monolayers (54). In similarity with high-perfor-

mance inorganic dielectrics, capacitance measurements pointed to the presence of "dead" interfacial capacitance, because the values of dielectric constant extracted from capacitors thinner than ~10 nm were up to 0.7 times lower than the bulk value. Simple geometric model based on the incommensurability between metal electrode and polymer film has been shown to be capable of adequately accounting for this effect. This suggests that minimization of interfacial roughness (e.g., by using more compact hyperbranched macromolecules with narrower molecular weight distribution) could be a viable approach to coping with this detrimental effect common to nanoscale capacitors. Controlled radical polymerizations such as ATRP appear to be particularly well-suited for such a task.

**Acknowledgment.** The authors thank the National Science Foundation (09-69301) and the members of the CRP Consortium at Carnegie Mellon University for their financial support. Also, Dr. James Spanswick and Dr. Yungwan Kwak are greatly appreciated for their thorough comments and discussions.

**Supporting Information Available:** Experimental details, detailed description of synthetic strategies, additional results of physical property measurements, and the derivation of eq 1 (PDF). This material is available free of charge via the Internet at http://pubs.acs.org.

## REFERENCES AND NOTES

(1) Loschonsky, S.; Shroff, K.; Worz, A.; Prucker, O.; Ruhe, J.; Biesalski, M. *Biomacromolecules* **2008**, *9*, 543–552.
(2) Ryu, D. Y.; Shin, K.; Drockenmuller, E.; Hawker, C. J.; Russell, T. P. *Science* **2005**, *308*, 236–239.
(3) Benhabbour, S. R.; Sheardown, H.; Adronov, A. *Biomaterials* **2008**, *29*, 4177–4186.
(4) Boulares-Pender, A.; Prager-Duschke, A.; Elsner, C.; Buchmeiser, M. R. *J. Appl. Polym. Sci.* **2009**, *112*, 2701–2709.
(5) Fang, F.; Szleifer, I. *Proc. Natl. Acad. Sci. U.S.A.* **2006**, *103*, 5769–5774.
(6) Luo, Y.; Li, Y.; Jia, X.; Yang, H.; Yang, L.; Zhou, Q.; Wei, Y. *J. Appl. Polym. Sci.* **2003**, *89*, 1515–1519.
(7) Nithyanandhan, J.; Jayaraman, N.; Davis, R.; Das, S. *Chem. - Eur. J.* **2004**, *10*, 689–698.
(8) Lin, W.; Sun, W.; Yang, J.; Sun, Q.; Shen, Z. *J. Phys. Chem. C* **2009**, *113*, 16884–16895.
(9) Perez, G. P.; Yelton, W. G.; Cernosek, R. W.; Simonson, R. J.; Crooks, R. M. *Anal. Chem.* **2003**, *75*, 3625–3630.
(10) Priya, D. N.; Modak, J. M.; Raichur, A. M. *ACS Appl. Mater. Interfaces* **2009**, *1*, 2684–2693.
(11) Pinto, M. R.; Kristal, B. M.; Schanze, K. S. *Langmuir* **2003**, *19*, 6523–6533.
(12) Bertrand, P.; Jonas, A.; Laschewsky, A.; Legras, R. *Macromol. Rapid Commun.* **2000**, *21*, 319–348.
(13) Bhattacharya, A.; Misra, B. N. *Prog. Polym. Sci.* **2004**, *29*, 767–814.
(14) Viswanathan, K.; Long, T. E.; Ward, T. C. *J. Polym. Sci., Part A: Polym. Chem.* **2005**, *43*, 3655–3666.
(15) Pallandre, A.; de Lambert, B.; Attia, R.; Jonas, A. M.; Viovy, J. L. *Electrophoresis* **2006**, *27*, 584–610.
(16) Vestberg, R.; Malkoch, M.; Kade, M.; Wu, P.; Fokin, V. V.; Sharpless, K. B.; Drockenmuller, E.; Hawker, C. J. *J. Polym. Sci., Part A: Polym. Chem.* **2007**, *45*, 2835–2846.
(17) Quinn, J. F.; Johnston, A. P. R.; Such, G. K.; Zelikin, A. N.; Caruso, F. *Chem. Soc. Rev.* **2007**, *36*, 707–718.
(18) Walheim, S.; Boltau, M.; Mlynek, J.; Krausch, G.; Steiner, U. *Macromolecules* **1997**, *30*, 4995–5003.
(19) Becker, J.; Grun, G.; Seemann, R.; Mantz, H.; Jacobs, K.; Mecke, K. R.; Blossey, R. *Nat. Mater.* **2003**, *2*, 59–63.
(20) Prucker, O.; Naumann, C. A.; Ruhe, J.; Knoll, W.; Frank, C. W. *J. Am. Chem. Soc.* **1999**, *121*, 8766–8770.
(21) Chan, E. W. L.; Lee, D.-C.; Ng, M.-K.; Wu, G.; Lee, K. Y. C.; Yu, L. *J. Am. Chem. Soc.* **2002**, *124*, 12238–12243.
(22) Fan, X.; Lin, L.; Dalsin, J. L.; Messersmith, P. B. *J. Am. Chem. Soc.* **2005**, *127*, 15843–15847.
(23) Chua, L. L.; Ho, P. K. H.; Sirringhaus, H.; Friend, R. H. *Appl. Phys. Lett.* **2004**, *84*, 3400–3402.
(24) Gao, C.; Yan, D. *Prog. Polym. Sci.* **2004**, *29*, 183–275.
(25) Gao, H.; Matyjaszewski, K. *Prog. Polym. Sci.* **2009**, *34*, 317–350.
(26) Ishizu, K.; Takahashi, D.; Takeda, H. *Polymer* **2000**, *41*, 6081–6086.
(27) Nunez, C. M.; Chiou, B.-S.; Andrady, A. L.; Khan, S. A. *Macromolecules* **2000**, *33*, 1720–1726.
(28) Du, J.; Chen, Y. *Macromolecules* **2004**, *37*, 6322–6328.
(29) Lu, X.; Xin, Z. *Colloid Polym. Sci.* **2007**, *285*, 599–604.
(30) Braunecker, W. A.; Matyjaszewski, K. *Prog. Polym. Sci.* **2007**, *32*, 93–146.
(31) *Handbook of Radical Polymerization*; Matyjaszewski, K.; Davis, T. P., Eds.; Wiley Interscience: Hoboken, NJ, 2002.
(32) *Macromolecular Engineering: From Precise Macromolecular Synthesis to Macroscopic Materials Properties and Applications*; Matyjaszewski, K.; Gnanou, Y.; Leibler, L., Eds.; Wiley-VCH: Weinheim, Germany, 2007.
(33) Frechet, J. M. J.; Henmi, M.; Gitsov, I.; Aoshima, S.; Leduc, M. R.; Grubbs, R. B. *Science* **1995**, *269*, 1080–1083.
(34) Matyjaszewski, K.; Gaynor, S. G. *Macromolecules* **1997**, *30*, 7042–7049.
(35) Matyjaszewski, K.; Pyun, J.; Gaynor, S. G. *Macromol. Rapid Commun.* **1998**, *19*, 665–670.
(36) Wang, J. S.; Matyjaszewski, K. *J. Am. Chem. Soc.* **1995**, *117*, 5614–5615.
(37) Patten, T. E.; Xia, J. H.; Abernathy, T.; Matyjaszewski, K. *Science* **1996**, *272*, 866–868.
(38) Tsarevsky, N. V.; Matyjaszewski, K. *Chem. Rev.* **2007**, *107*, 2270–2299.
(39) Ouchi, M.; Terashima, T.; Sawamoto, M. *Chem. Rev.* **2009**, *109*, 4963–5050.
(40) Matyjaszewski, K.; Tsarevsky, N. V. *Nat. Chem.* **2009**, *1*, 276–288.
(41) Jakubowski, W.; Matyjaszewski, K. *Macromolecules* **2005**, *38*, 4139–4146.
(42) Matyjaszewski, K.; Jakubowski, W.; Min, K.; Tang, W.; Huang, J. Y.; Braunecker, W. A.; Tsarevsky, N. V. *Proc. Natl. Acad. Sci. U.S.A.* **2006**, *103*, 15309–15314.
(43) Jakubowski, W.; Matyjaszewski, K. *Angew. Chem., Int. Ed.* **2006**, *45*, 4482–4486.
(44) Isaure, F.; Cormack, P. A. G.; Sherrington, D. C. *J. Mater. Chem.* **2003**, *13*, 2701–2710.
(45) Isaure, F.; Cormack, P. A. G.; Sherrington, D. C. *Macromolecules* **2004**, *37*, 2096–2105.
(46) Wong, K. H.; Stenzel, M. H.; Duvall, S.; Ladouceur, F.o. *Chem. Mater.* **2010**, *22*, 1878–1891.
(47) Gao, H.; Min, K.; Matyjaszewski, K. *Macromolecules* **2009**, *42*, 8039–8043.
(48) Van Camp, W.; Gao, H.; Du Prez, F. E.; Matyjaszewski, K. *J. Polym. Sci., Part A: Polym. Chem.* **2010**, *48*, 2016–2023.
(49) Litvinenko, G. I.; Simon, P. F. W.; Müller, A. H. E. *Macromolecules* **1999**, *32*, 2410–2419.
(50) Stengel, M.; Spaldin, N. A. *Nature* **2006**, *443*, 679–682.
(51) Sinnamon, L. J.; Saad, M. M.; Bowman, R. M.; Gregg, J. M. *Appl. Phys. Lett.* **2002**, *81*, 703–705.
(52) Basceri, C.; Streiffer, S. K.; Kingon, A. I.; Waser, R. *J. Appl. Phys.* **1997**, *82*, 2497–2504.
(53) Hickmott, T. W. *J. Appl. Phys.* **2001**, *89*, 5502–5508.
(54) Facchetti, A.; Yoon, M. H.; Marks, T. J. *Adv. Mater.* **2005**, *17*, 1705–1725.

AM100463Z